

Production and ratio of π , K , p and Λ in Pb + Pb collisions at $\sqrt{s_{NN}} = 2.76$ TeV

S. Zhang, L. X. Han, Y. G. Ma*, J. H. Chen, and C. Zhong

Shanghai Institute of Applied Physics, Chinese Academy of Sciences, Shanghai 201800, China

(Dated: July 25, 2018)

The particle production and their ratios for π , K , p , and Λ are studied in Pb + Pb collisions at $\sqrt{s_{NN}} = 2.76$ TeV based on a blast-wave model with thermal equilibrium mechanism. The transverse momentum spectra of the above mentioned particles at the kinetic freeze-out stage are discussed. The modification of the inverse slope of pion transverse momentum spectrum due to resonance decay has also been investigated. In addition, we found that the anti-particles to particles ratio as well as kaons to pions ratio agree with the data by the LHC-ALICE Collaboration reasonably well, while the p/π ratio is overestimated by a factor of 1.5, similar to those from other thermal model calculations. It is found that the ratios of p/π and K/π are dominated by the radial flow but slightly affected by the baryon chemical potential. Our study thus constrains the parameters at the chemical and kinetic freeze-out stages within the framework of thermal model in Pb + Pb collisions at $\sqrt{s_{NN}} = 2.76$ TeV, and will help better understand the properties of the dense and hot matter created in high-energy heavy-ion collisions at freeze-out stage.

PACS numbers: 25.75.Gz, 12.38.Mh, 24.85.+p

I. INTRODUCTION

Ultra-relativistic heavy-ion collisions opens a window for studying the properties of the Quark-Gluon Plasma (QGP) which was predicted by quantum chromodynamics (QCD) [1]. This exotic matter is believed to be produced in the early stage of central Au + Au collisions at the top energy in the Relativistic Heavy-Ion Collider (RHIC) at Brookhaven National Laboratory [2]. The sufficient experimental evidences [3] support that the new hot and dense QCD matter is not an ideal gas but instead a strongly interacting dense partonic matter named as sQGP under extreme temperature and energy density. The collective properties of the exotic matter created at RHIC can be investigated through transverse momentum (p_T) distribution and elliptic flow of identified particles, and so far people have found that this matter behaves as a nearly ideal fluid [4]. Recently, experimental results in Pb + Pb collisions at $\sqrt{s_{NN}} = 2.76$ TeV in the Large Hadron Collider (LHC) are also reported by the ALICE Collaboration [5–8]. This provides another opportunity to investigate the bulk properties of the exotic QCD matter as an expanding fireball created in heavy-ion collisions at a higher energy, such as its baryon chemical potential μ_B , chemical freeze-out temperature T_{ch} , and kinetic freeze-out temperature T_{kin} as well as radial expansion velocity $\langle\beta_T\rangle$, etc.

Relativistic hydrodynamics and thermal models are very successful in describing particle productions at the freeze-out stage. The viscous hydrodynamic model VISH2+1 [9] has successfully described the transverse momentum distributions of π and K . Similar model named HKM [10] coupling with UrQMD for the hadronic

scattering stage can also reproduce the yields and distributions of particles such as π , K , and p . The EPOS model [11] aims at describing complete transverse momentum distributions of particles within the same dynamical picture. A multiphase transport (AMPT) model has been reconfigured to reproduce the p_T distribution of charged particles as well as their elliptic flow in Pb + Pb collisions at $\sqrt{s_{NN}} = 2.76$ TeV [12]. Besides the studies from hydrodynamics or transport models mentioned about, the thermal model has also successfully described the production of particles in heavy-ion collisions with a few parameters such as the chemical freeze-out temperature, the baryon chemical potential, and the fireball volume [13]. From particle ratios, the thermal model [14] can be used to obtain the chemical freeze-out properties, such as the chemical freeze-out temperature T_{ch} as well as the baryon (μ_B) and the strangeness (μ_S) chemical potential. By fitting the transverse momentum distribution, the blast-wave model [15] has often been used to extract the kinetic freeze-out properties such as the kinetic freeze-out temperature T_{kin} and the radial flow velocity $\langle\beta_T\rangle$. These thermal models have also been applied in experimental analysis [8, 16] to study the chemical and kinetic freeze-out properties. Retière and Lisa [17] have explored in detail an analytic parametrization of the freeze-out configuration and investigated the spectra, the collective flow, and the HBT correlation of hadrons produced in head-on collisions at top RHIC energy. In addition, the DRAGON model [18] and the THERMINATOR2 [19] model have also been developed to study the phase-space distribution of produced hadrons at freeze-out stage.

Due to the complicated initial condition and dynamical evolution in heavy-ion collisions, it is very likely that the particle production can be explained with different parameter sets of temperature, chemical potential, and radial flow. The values of these parameters give the acceptable range of the system properties at freeze-out

*Author to whom all correspondence should be addressed: ygma@sinap.ac.cn

stage. The results in this paper come from the fitting based on the blast-wave model with thermal equilibrium mechanism. Transverse momentum (p_T) distributions of charged hadrons (π , K , and p) and Λ hyperon in Pb + Pb collisions at $\sqrt{s_{NN}} = 2.76$ TeV are presented. The effect from resonance decay to the p_T spectrum of pions will also be discussed. The inverse slope parameter of the p_T spectrum is extracted for each particle species at various centralities. The multiplicities of anti-particles and particles become similar by tuning baryon chemical potential to about 0.1 MeV at LHC energy. The inclusive yields of charged hadrons and hyperons normalized to the pion yield in 0 – 5% centrality are compared with the experimental results. From the transverse momentum dependence of mixed ratios of p/π and K/π , the radial flow effect on the mass ordering of p_T distribution is investigated. The calculated results agree pretty well with the experimental measurements by the LHC-ALICE

Collaboration, and a reasonable range of parameters at the chemical and kinetic freeze-out stages is discussed for the thermalized system at LHC energy.

II. BLAST-WAVE MODEL WITH THERMAL EQUILIBRIUM MECHANISM

As discussed above, thermal model can describe particle yield by adjusting parameters such as the chemical freeze-out temperature T_{ch} , the baryon chemical potential μ_B , the strangeness chemical potential μ_S , and the system volume V . On the other hand, one can extract these quantities at chemical freeze-out stage through particle ratios. The particle density of species i can be expressed as [13, 14, 18]

$$\begin{aligned} n_i(T_{ch}, \mu_B, \mu_S) &= g_i \int \frac{d^3p}{(2\pi)^3} \left[\exp \left(\frac{\sqrt{p^2 + m_i^2} - (\mu_B B_i + \mu_S S_i)}{T_{ch}} \right) \mp 1 \right]^{-1} \\ &= I \left(g_i, \frac{m_i}{T_{ch}} \right) \sum_{n=1} (\pm 1)^{n+1} \exp \left(n \frac{(\mu_B B_i + \mu_S S_i)}{T_{ch}} \right), \\ I \left(g_i, \frac{m_i}{T_{ch}} \right) &= g_i \int \frac{d^3p}{(2\pi)^3} \left[\sum_{n=1} (\pm 1)^{n+1} \exp \left(-n \frac{\sqrt{p^2 + m_i^2}}{T_{ch}} \right) \right], \end{aligned} \quad (1)$$

with the upper (lower) sign for bosons (fermions) and g_i being the degeneracy factor. Assuming that the chemical equilibrium condition is satisfied, Eq. (1) essentially determines the fraction of particle species i . Within the framework of the blast-wave model, the fireball created in

high-energy heavy-ion collisions is assumed to be in local thermal equilibrium and expands at a four-component velocity u_μ . The phase-space distribution of hadrons emitted from the expanding fireball can be expressed as a Wigner function [17–19]

$$S(x, p) d^4x = \frac{2s + 1}{(2\pi)^3} m_t \cosh(y - \eta) \exp \left(-\frac{p^\mu u_\mu}{T_{kin}} \right) \Theta(1 - \tilde{r}(r, \phi)) H(\eta) \delta(\tau - \tau_0) d\tau \tau d\eta r dr d\phi, \quad (2)$$

where s , y , and m_t are respectively the spin, rapidity, and transverse mass of the hadron, and p_μ is the four-component momentum. Equation (2) is formulated in a Lorentz covariant way, r and ϕ are the polar coordinates, and η and τ are the pseudorapidity and the proper time, respectively. \tilde{r} is defined as

$$\tilde{r} = \sqrt{\frac{(x^1)^2}{R^2} + \frac{(x^2)^2}{R^2}}, \quad (3)$$

with (x^1, x^2) standing for the coordinates in the transverse plane and R being the average transverse radius.

The kinetic freeze-out temperature T_{kin} and the radial flow parameter ρ_0 are important in determining the transverse momentum spectrum, with the latter affecting the four-component velocity field. Since we are only interested in the p_T spectrum at mid-rapidity, the pseudorapidity distribution $H(\eta)$ is not important. The p_T spectrum can then be written as

$$\frac{dN}{2\pi p_T dp_T} = \int S(x, p) d^4x, \quad (4)$$

and the fraction of particle species i and its phase-space distribution can be calculated from Eqs. (1) and (4).

III. TRANSVERSE MOMENTUM SPECTRA

The collective properties of the hot and dense matter created in ultra-relativistic heavy-ion collisions at freeze-out stage can be studied through transverse momentum (p_T) distributions of identified particles. Figure 1 shows the p_T distributions of π , K , p , and Λ in central and peripheral Pb + Pb collisions at $\sqrt{s_{NN}} = 2.76$ TeV by using the blast-wave model with thermal equilibrium mechanism. The parameters of kinetic temperature (T_{kin}) and radial flow parameter (ρ_0) used in the calculation are also shown in Fig. 1. The spectra become stiffer with increasing ρ_0 and T_{kin} , and the results imply that the transverse momentum distribution is more sensitive to the radial flow parameter than to the kinetic freeze-out temperature. The ranges of the chemical and kinetic temperature (T_{ch} and T_{kin}) as well as the chemical potential (μ_B and μ_S) are consistent with those from other model calculations [9, 13] and the experimentally estimated values [8, 20]. The radial flow

$$\langle\beta_T\rangle = \int \operatorname{arctanh}\left(\rho_0 \frac{r}{R}\right) r dr / \int r dr \quad (5)$$

is related to the maximum flow rapidity

$$\rho = \tilde{r} [\rho_0 + \rho_a \cos(2\phi)]. \quad (6)$$

The results are independent of ρ_a as after integration the ϕ dependence is averaged out. The parameter ρ_0 from our analysis is comparable to that extracted from the experimental data [7, 8, 20, 21] except for Λ in central collisions (0 – 10%). In addition, we can see that the effect from the radial flow parameter ρ_0 on the spectra is more significant than the kinetic freeze-out temperature T_{kin} . The results show that the inverse slopes T_{loc} increase with ρ_0 in the range of ρ_0 from 0.9 to 1.1, which is consistent with the previous calculation using the blast-wave model [17].

The properties of a thermalized system can be extracted from the spectra of identified particles. A rough description of spectra slope can be obtained by an exponential or a power-law fit. From Fig. 1, we can see that the spectra of identified particles become stiffer from peripheral collisions to central collisions. Experimental data have demonstrated that there is no obvious onset of the power-law tail at high p_T as observed in pp collisions [24], but in central collisions the spectra keep an almost exponential shape in a wide p_T range. The transverse momentum dependence of the slope parameters can display more clearly the trend of the spectra changing from the exponential pattern to the power-law one. Figure 2 shows the local inverse slope T_{loc} of the spectra as a function of p_T , which is calculated by fitting the spectra

with the following function [8]

$$\frac{1}{p_T} \frac{dN}{d_{p_T}} \propto e^{-p_T/T_{loc}}. \quad (7)$$

It is seen that the inverse slopes of identified particles p_T spectra have a similar trend of p_T dependence to the experimental results [8]. The inverse slopes of the p_T spectra for K , p , and Λ decrease with the increasing transverse momentum, and this is more obvious for central collisions. In addition, they don't change with increasing p_T above a certain value of the transverse momentum, which is about 1 GeV/c for K and 2 GeV/c for p and Λ . It is also seen that T_{loc} for protons and kaons converges to a similar value of 0.45 GeV/c at high p_T . In peripheral collisions from the ALICE [8] data, a modest increase of T_{loc} is seen at the highest p_T , showing the onset of a power-law behavior. The above experimental results thus indicate that the system becomes more thermalized with sufficient particle interaction in central collisions in comparison with peripheral collisions.

For pions, however, the inverse slopes increase with p_T in both central and peripheral collisions, opposite to the trend observed for protons and kaons. At high p_T , the power-law rise is more suppressed in central collisions in comparison with peripheral ones. The calculated results are consistent with the experimental ones except at high p_T ($p_T > 1.5$ GeV/c) in peripheral collisions. The pions from resonances decay contribute to the distribution at low transverse momenta, and this might be the reason why a different trend of pion spectrum compared to protons and kaons is observed [11, 15, 16]. The contribution of resonance decay to the total pion yield is estimated in this calculation by distinguishing directly produced pions from the fireball and pions from resonance decay, and they are compared in Fig. 3. In central collisions (left top), the yield of pions from resonance decay is higher than those from direct production, and this is more pronounced in the top of the right figures, i.e., the fraction of the contribution from resonance decay in the total yield grows with increasing p_T from 60% to 80%. In peripheral collisions (left and right bottom), however, this fraction decreases with increasing p_T from 60% to 40%, and the directly produced pion is dominant above $p_T \sim 2$ GeV/c. This implies that the contribution of the resonance decay is dominant in central collisions but only important at low p_T in peripheral collisions.

IV. PARTICLE RATIO ANALYSIS

The estimate of the baryon chemical potential μ_B gives the value of about zero from the similar multiplicity of anti-particles and particles measured by the ALICE Collaboration [8]. The anti-particles to particles ratio can be approximately deduced from Eq. (1) by neglecting the

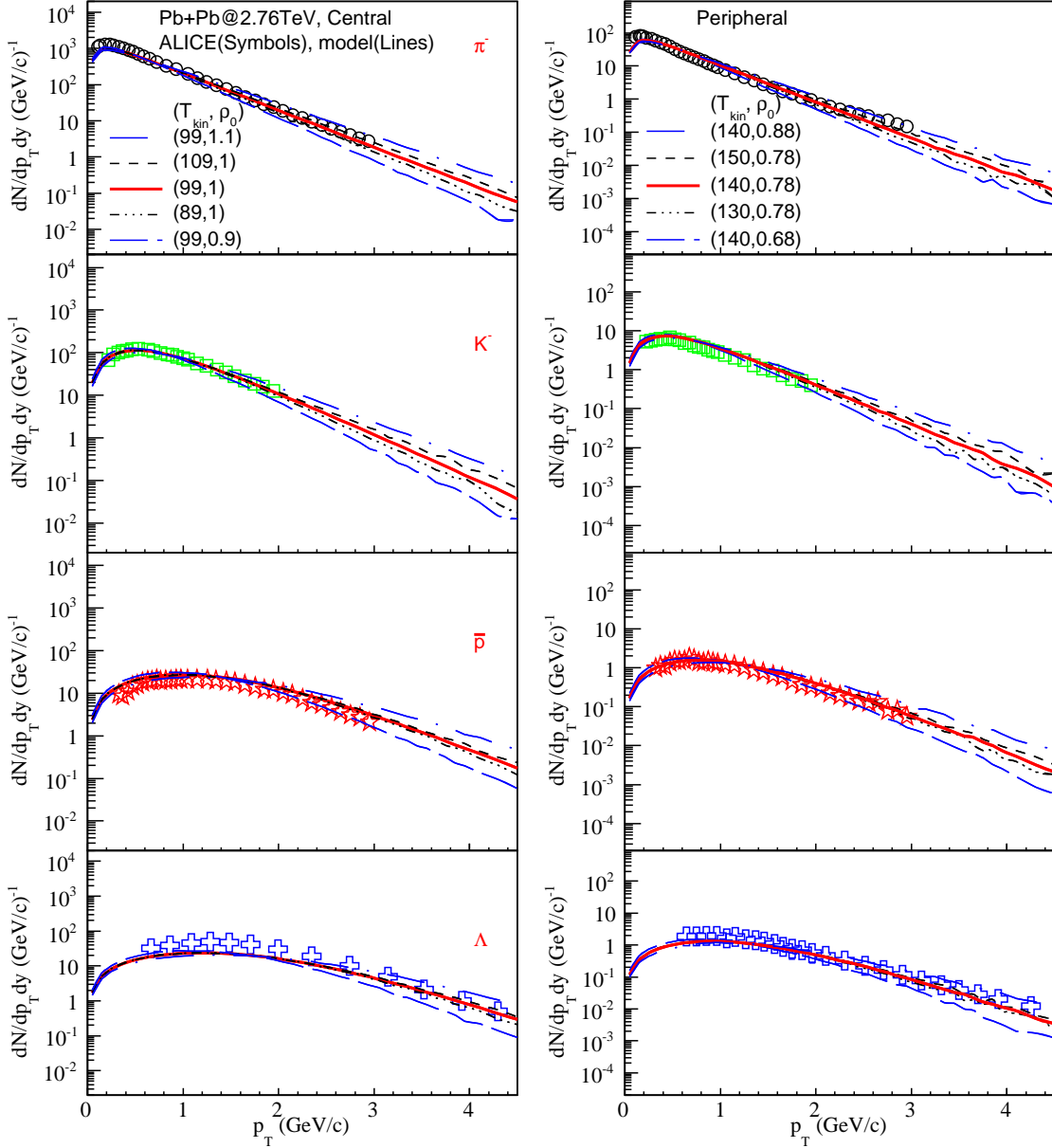


FIG. 1: (Color online) Transverse momentum (p_T) distribution of π , K , p , and Λ in central and peripheral collisions. Lines: model calculations with $\mu_B = 0.1$ MeV, $\mu_S = 0.001$ MeV, and $T_{ch} = 160$ MeV for central collisions and $T_{ch} = 150$ MeV for peripheral collisions; Symbols: ALICE data [8, 21–23], collision centrality 0 – 5% (left column) and 70 – 80% (right column) for π^- , K^- , and p , and 0 – 10% (left column) and 60 – 80% (right column) for Λ . T_{kin} is in MeV and ρ_0 is dimensionless.

second- and higher-order terms, i.e.,

$$\begin{aligned} \frac{\bar{n}_i}{n_i} &\approx \exp\left(\frac{\mu_B(\bar{B}_i - B_i) + \mu_S(\bar{S}_i - S_i)}{T_{ch}}\right) \\ &= \exp\left(-2\frac{\mu_B|B_i| + \mu_S|S_i|}{T_{ch}}\right). \end{aligned} \quad (8)$$

From Eq. (8), it can be seen that the multiplicity ratio of anti-particle to particle is affected by the chemical properties of the bulk matter such as T_{ch} , μ_B , and μ_S . Table. I gives the multiplicity ratios of anti-particles to

particles from different parameter sets used in the calculation. It is seen that there is minor effect from the chemical freeze-out temperature T_{ch} and the strangeness chemical potential μ_S on the ratio. However, the baryon chemical potential μ_B dominates the ratio of anti-baryon to baryon (\bar{p}/p and $\bar{\Lambda}/\Lambda$). It is obviously seen that the ratios are compatible with unit for centralities of 0 – 5% and 70 – 80% with the chemical potential μ_B and μ_S close to zero, consistent with the experimental observation [8]. This means that the experimental results can be well de-

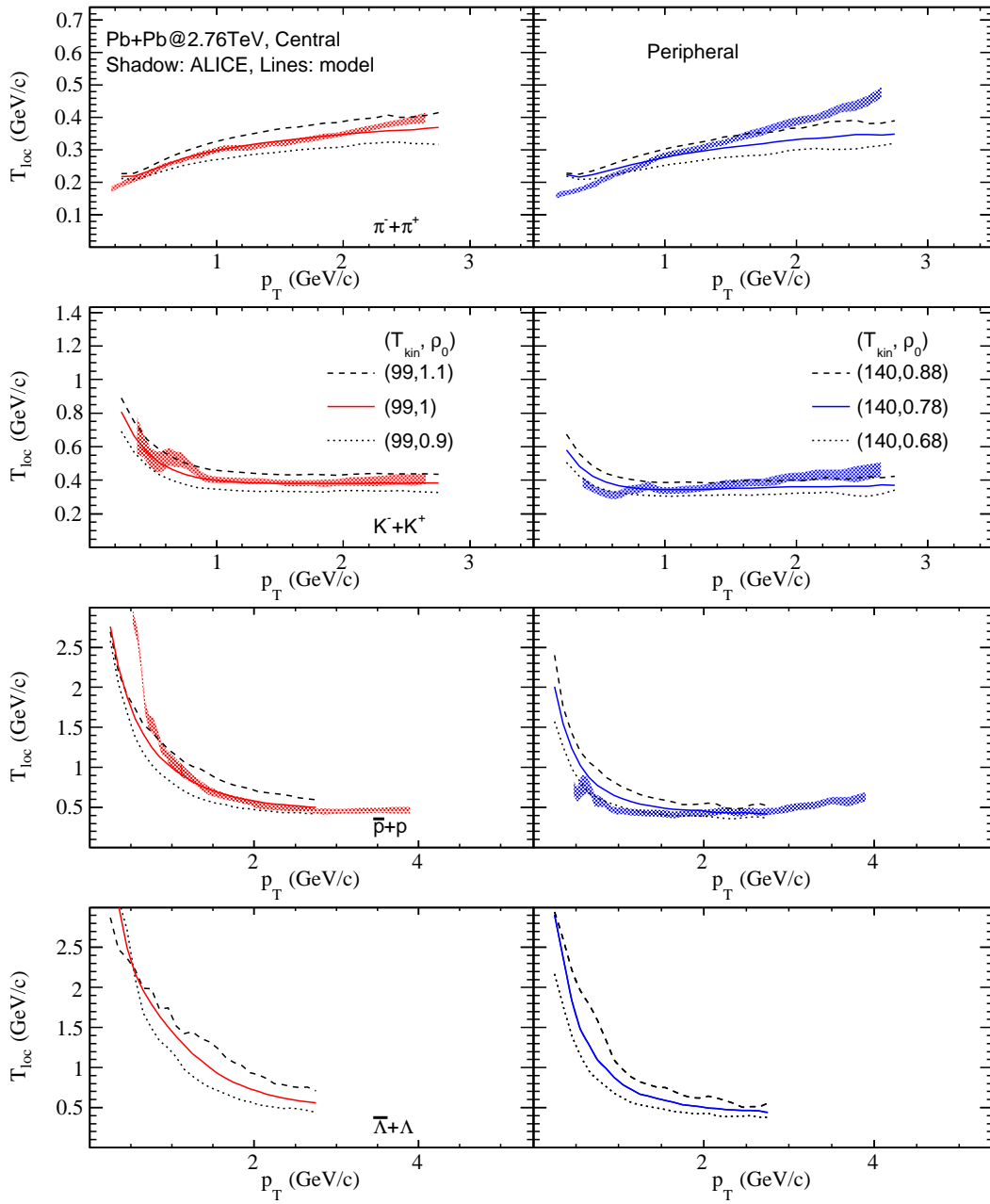


FIG. 2: (Color online) Local slopes of the p_T distributions for π , K , p , and Λ including their anti-particles as a function of p_T in central and peripheral collisions. Lines: model calculations with $\mu_B = 0.1$ MeV, $\mu_S = 0.001$ MeV, and $T_{ch} = 160$ MeV for central collisions and $T_{ch} = 150$ MeV for peripheral collisions; Shadow: the ALICE data [8] for collision centrality 0 – 5% (left column) and 70 – 80% (right column). T_{kin} is in MeV and ρ_0 is dimensionless.

scribed by thermal equilibrium mechanism, and this implies that the hot and dense matter created at LHC energy has nearly equal amount of matter and anti-matter with the chemical potential close to zero.

The accurate ratio of inclusive yields of particles to those of π^+ can be deduced from Eq. (1) as done in Eq. (8)

$$\frac{n_i}{n_{\pi^+}} = \frac{I(g_i, m_i/T_{ch})}{I(g_{\pi^+}, m_{\pi^+}/T_{ch})} \exp\left(\frac{\mu_B B_i + \mu_S S_i}{T_{ch}}\right). \quad (9)$$

The ratio of inclusive particle yields to that of π^+ is thus determined by T_{ch} , μ_B , and μ_S in addition to the intrinsic parameters of mass m_i and the degeneracy factor g_i . Figure 4 shows particle yield ratios of hadrons to π^+ in 0 – 5% centrality and they are compared with the experimental results [21, 26]. Within the range of the chemical freeze-out temperature T_{ch} and the chemical potentials μ_B and μ_S as shown in Fig. 4, particle yield ratios of most hadrons to π^+ in this calculation are consistent with those in Ref. [13]. However, the thermal model can not

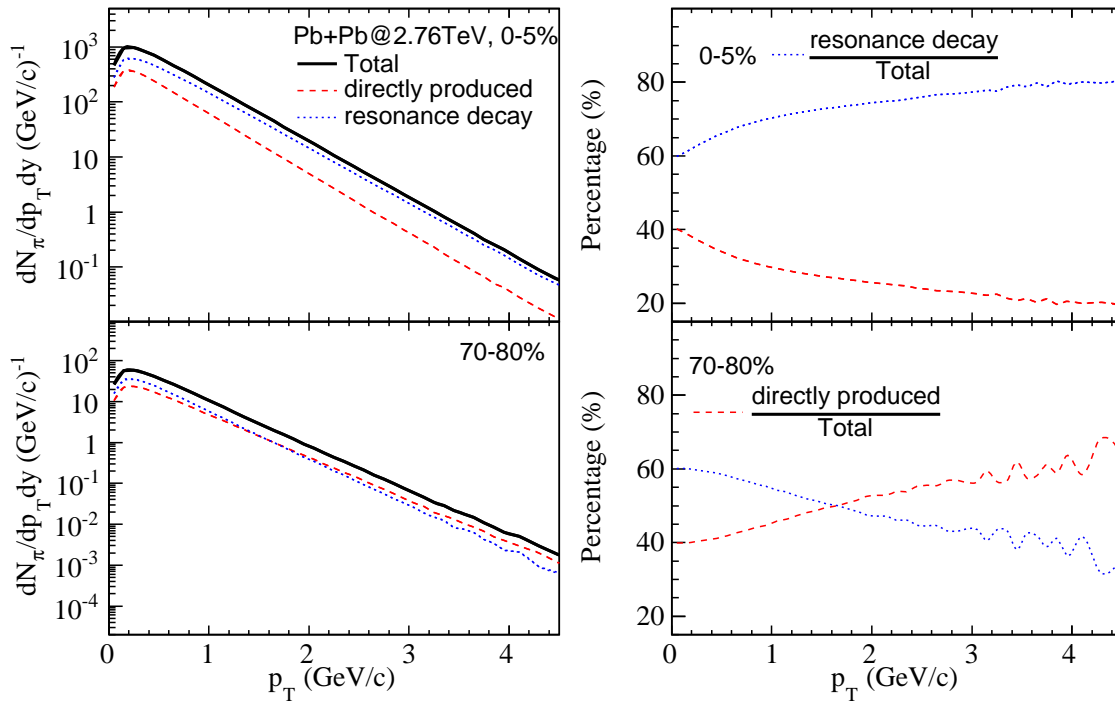


FIG. 3: (Color online) Comparing the pion p_T spectrum from direct production and resonance decay from model calculations with $(T_{ch}, \mu_B, \mu_S, T_{kin}, \rho_0) = (160, 0.1, 0.001, 99, 1)$ (all in MeV except that ρ_0 is dimensionless) for central collisions and $(T_{ch}, \mu_B, \mu_S, T_{kin}, \rho_0) = (150, 0.1, 0.001, 140, 0.78)$ for peripheral collisions; Left: Pions spectra from direct production and total yield in central and peripheral collisions; Right: The ratios of pions from resonance decay and direct production to the total yield as a function of p_T in central and peripheral collisions.

TABLE I: Ratios of anti-particles to particles for π , K , p , and Λ in central and peripheral collisions. Results from model calculations with $T_{kin} = 99$ MeV and $\rho_0 = 1$ for central collisions and $T_{kin} = 140$ MeV and $\rho_0 = 0.78$ for peripheral collisions are compared with the ALICE data [8] for collision centrality 0 – 5% and 70 – 80%.

(T_{ch}, μ_B, μ_S) (MeV)	π^-/π^+	K^-/K^+	\bar{p}/p	$\bar{\Lambda}/\Lambda$
Centrality (0-5%), ALICE	0.998	1.00	0.971	-
(160, 0.1, 0.001)	0.99	0.99	1.00	0.99
(150, 0.1, 0.001)	0.99	0.99	1.00	0.98
(170, 0.1, 0.001)	0.99	0.99	1.00	1.00
(160, 0.1, 0.1)	0.99	0.99	1.00	0.99
(160, 10, 0.001)	0.99	0.99	0.88	0.88
Centrality (70-80%), ALICE	0.994	1.00	1.033	-
(150, 0.1, 0.001)	0.997	0.995	1.003	0.997
(140, 0.1, 0.001)	1.000	0.998	1.006	1.018
(160, 0.1, 0.001)	0.995	0.993	0.994	0.994
(150, 0.1, 0.1)	0.997	0.992	0.992	0.997
(150, 10, 0.001)	0.998	0.994	0.879	0.877

reproduce the yield of protons ($T_{ch} = 150$ MeV) and Λ hyperons ($T_{ch} = 160$ MeV) with the same parameters, and it calls for more theoretical works for particle production mechanism, which is beyond what we have in the present paper.

The transverse momentum dependence of mixed ratio of p/π (stands for $(p + \bar{p})/(\pi^+ + \pi^-)$) and K/π (stands

for $(K^+ + K^-)/(\pi^+ + \pi^-)$) will be affected by both chemical freeze-out properties and kinetic freeze-out properties. From the above discussion, it is known that the slope of particle spectra and their ratios are mainly determined by the radial flow parameter ρ_0 and the baryon chemical potential μ_B , respectively. It will be interesting to investigate these ratios in different ranges of ρ_0 and

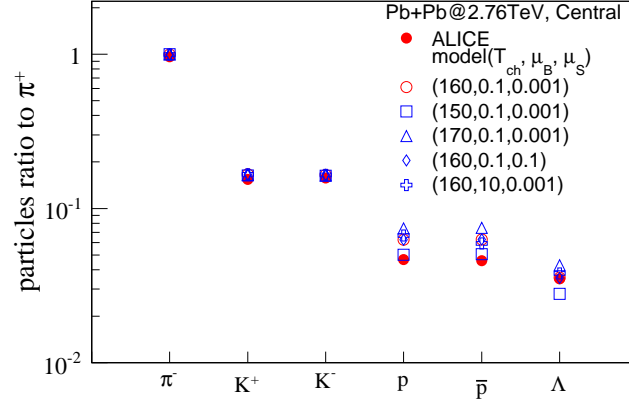


FIG. 4: (Color online) Ratio of inclusive yields of particles to π^+ compared with the LHC-ALICE data for central (0 – 5%) collisions [21, 26]. T_{ch} , μ_B , and μ_S are all in MeV.

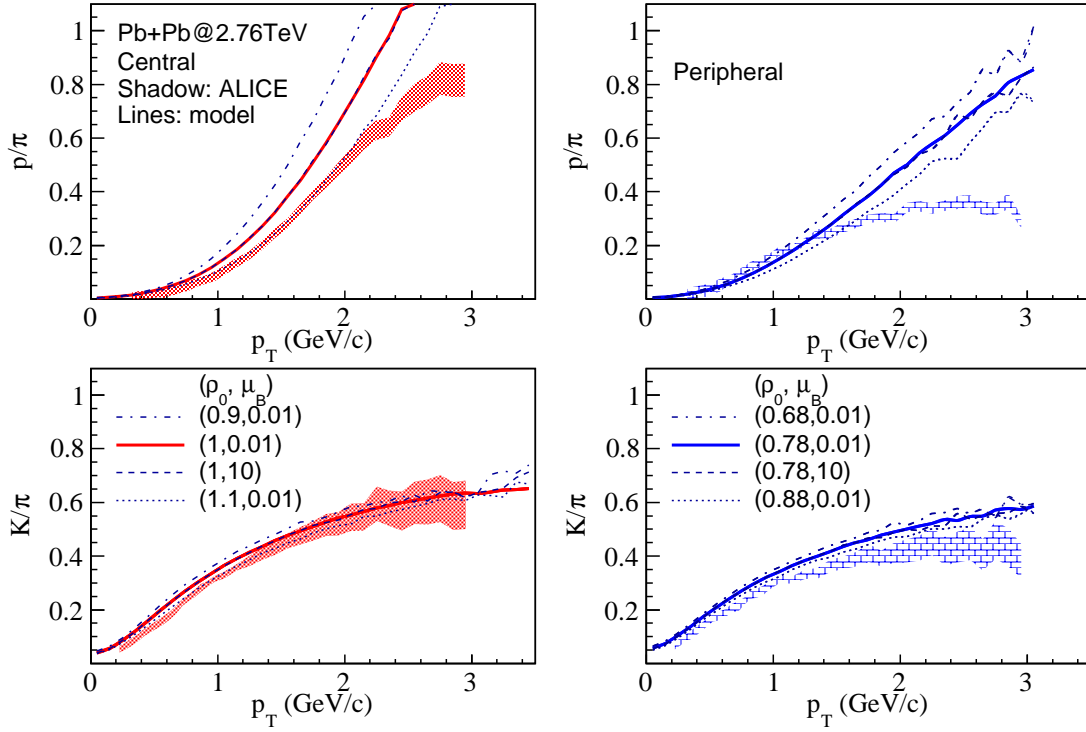


FIG. 5: (Color online) Ratios of p/π (stands for $(p + \bar{p})/(\pi^+ + \pi^-)$) and K/π (stands for $(K^+ + K^-)/(\pi^+ + \pi^-)$) as a function of p_T in central and peripheral collisions. Lines: model calculations with $\mu_S = 0.001$ MeV, $T_{ch} = 160$ MeV and $T_{kin} = 99$ MeV for central collisions, and $T_{ch} = 150$ MeV and $T_{kin} = 140$ MeV for peripheral collisions; Shadow: the ALICE data [8] for collision centrality 0 – 5% (left column) and 70 – 80% (right column). ρ_0 is dimensionless and μ_B is in MeV.

μ_B used above. The ratios of p/π and K/π as a function of p_T are shown in Fig. 5. It is seen that there is no significant effect from μ_B on the particle ratio, while a large radial flow parameter ρ_0 will reduce the ratios, especially for p/π . The effect from ρ_0 as well as the increasing trend of the ratios with transverse momentum are intrinsic features of hydrodynamical models, where heavier particles are pushed to higher p_T by the collective motion of radial flow. The increasing trend of both

ratios with p_T is more pronounced in central collisions and this is consistent with the LHC-ALICE results [8]. However, the ratios from our calculations are higher than the experimental results, except for K/π in central collisions. For the p/π ratio, the result from our calculations and those by other models [10, 25] overestimate the value measured by the LHC-ALICE Collaboration [8].

V. SUMMARY

The particle yield and their ratios of π , K , p , and Λ in Pb + Pb collisions at $\sqrt{s_{NN}} = 2.76$ TeV have been investigated based on the blast-wave model with thermal equilibrium mechanism. A reasonable range of the parameters at chemical and kinetic freeze-out stages in our calculation is selected to study the thermalized system at LHC energy. The transverse momentum spectra demonstrate some thermal and dynamical properties of the system, such as the radial flow, the chemical and kinetic temperatures, and the baryon (strangeness) chemical potential. Similar to the early findings, the slope of spectra is dominated by the radial flow parameter ρ_0 , while the anti-particles to particles ratio is essentially controlled by the baryon chemical potential, and the transverse momentum dependence of mixed ratios of p/π and K/π are only affected by ρ_0 . It is found that the slopes of K and p spectra becomes independent of p_T , which is about 0.4 GeV/c for K and 0.5 GeV/c for p , when the transverse momentum is above a certain value, which is about 1 GeV/c for K and 2 GeV/c for p , and this indicates an exponential shape of the p_T spectra at high p_T . The modification of the inverse slope of transverse momentum spectra for pions due to resonance decay has also

been investigated. The anti-particles to particles ratios are compatible with unity in central and peripheral collisions, which is consistent with the LHC results. This implies that the baryon chemical potential is almost zero at LHC energy. The inclusive yields of particles normalized to π^+ are comparable to those measured by the LHC-ALICE Collaboration but the p/π ratio is overestimated by a factor of 1.5 even though it is similar to those from other thermal model calculations. The ratios of p/π and K/π as a function of p_T are consistent with the results from hydrodynamical models, i.e., the radial flow can push heavier particles to higher p_T . Our detailed study helps better understand the chemical and kinetic properties of the hot and dense QCD matter created in heavy-ion collisions at LHC energy.

This work was supported in part by the Major State Basic Research Development Program in China under Contract No. 2014CB845400, the National Natural Science Foundation of China under contract Nos. 11035009, 11220101005, 11105207, 11275250, U1232206, the Knowledge Innovation Project of the Chinese Academy of Sciences under Grant No. KJCX2-EW-N01, and the "Shanghai Pujiang Program" under Grant No. 13PJ1410600.

-
- [1] F. Karsch, Nucl. Phys. A **698**, 199c (2002).
 [2] I. Arsene *et al.* (BRAHMS Collaboration), Nucl. Phys. A **757**, 1 (2005); B. B. Back *et al.* (PHOBOS Collaboration), *ibid.* A **757**, 28 (2005); J. Adames *et al.* (STAR Collaboration), *ibid.* A **757**, 102 (2005); S. S. Adler *et al.* (PHENIX Collaboration), *ibid.* A **757**, 184 (2005).
 [3] J. Adams *et al.* (STAR Collaboration), Phys. Rev. Lett. **95**, 122301 (2005); J. Adams *et al.* (STAR Collaboration), Phys. Rev. Lett. **93**, 252301 (2004); J. Adams *et al.* (STAR Collaboration), Phys. Lett. B **612**, 181 (2005); S. S. Adler *et al.* (PHENIX Collaboration), Phys. Rev. Lett. **96**, 012304 (2006); L. Adamczyk *et al.* (STAR Collaboration), Phys. Rev. C **86**, 054908 (2012).
 [4] P. Huovinen, P. Ruuskanen, Ann. Rev. Nucl. Part. Sci. **56**, 163 (2006); B. Müller, J. L. Nagle, Ann. Rev. Nucl. Part. Sci. **56**, 93 (2006); U. Heinz and R. Snellings, Ann. Rev. Nucl. Part. Sci. **63**, 123 (2013); C. M. Ko *et al.*, Nucl. Sci. Tech. **24**, 050525 (2013); J. Xu *et al.*, Phys. Rev. Lett. **112**, 012301 (2014); F. M. Liu, Nucl. Sci. Tech. **24**, 050524 (2013).
 [5] K. Aamodt *et al.* (ALICE Collaboration), Phys. Rev. Lett. **105**, 252301 (2010).
 [6] K. Aamodt *et al.* (ALICE Collaboration), Phys. Rev. Lett. **106**, 032301 (2011).
 [7] K. Aamodt *et al.* (ALICE Collaboration), Phys. Lett. B **696**, 30 (2011).
 [8] B. Abelev *et al.* (ALICE Collaboration), Phys. Rev. C **88**, 044910 (2013).
 [9] H. Song, S. A. Bass, U. Heinz, Phys. Rev. C **83**, 024912 (2011).
 [10] Iu. A. Karpenko, Yu. M. Sinyukov, K. Werner, Phys. Rev. C **87**, 024914 (2013); Yu. A. Karpenko, Yu. M. Sinyukov, J. Phys. G **38**, 124059 (2011).
 [11] K. Werner, I. Karpenko, M. Bleicher, T. Pierog, S. Porteboeuf-Houssais, Phys. Rev. C **85**, 064907 (2012).
 [12] J. Xu, C. M. Ko, Phys. Rev. C **83**, 034904 (2011); S. Pal and M. Bleicher, Phys. Lett. B **709**, 82 (2012).
 [13] P. Braun-Munzinger, K. Redlich, J. Stachel, arXiv:nucl-th/0304013v1; A. Andronic, P. Braun-Munzinger and J. Stachel, Phys. Lett. B **673**, 142 (2009).
 [14] P. Braun-Munzinger, J. Stachel, J. P. Wessels, N. Xu, Phys. Lett. B **344**, 43 (1995); P. Braun-Munzinger, J. Stachel, J. P. Wessels, N. Xu, Phys. Lett. B **365**, 1 (1996); P. Braun-Munzinger, I. Heppe, J. Stachel, Phys. Lett. B **465**, 15 (1999); N. Xu, M. Kaneta, Nucl. Phys. A **698**, 306 (2002).
 [15] E. Schnedermann, J. Sollfrank, U. Heinz, Phys. Rev. C **48**, 2462 (1993).
 [16] B. I. Abelev *et al.* (STAR Collaboration), Phys. Rev. C **79**, 034909 (2009).
 [17] F. Retière, M. A. Lisa, Phys. Rev. C **70**, 044907 (2004).
 [18] B. Tomášik, Comput. Phys. Commun. **180**, 1642 (2009).
 [19] M. Chojnacki, A. Kisiel, W. Florkowski, W. Broniowski, Comput. Phys. Commun. **183**, 746 (2012); A. Kisiel, T. Tahać, W. Broniowski, W. Florkowski, Comput. Phys. Commun. **174**, 669 (2006).
 [20] J. Adams *et al.* (STAR Collaboration), Phys. Rev. C **71**, 044906 (2005).
 [21] B. Müller, J. Schukraft, B. Wyslouch, arXiv:1202.3233v1.
 [22] M. Floris (for the ALICE Collaboration), J. Phys. G: Nucl. Part. Phys. **38**, 124025 (2011).
 [23] D. D. Chinellato (for the ALICE Collaboration), arXiv:1211.7298v1.

- [24] K. Aamodt et al. (ALICE Collaboration), Eur. Phys. J C **71**, 1 (2011).
[25] P. Bozek, arXiv:1111.4398.
[26] R. Preghenella (ALICE Collaboration), arXiv:1203.5904.